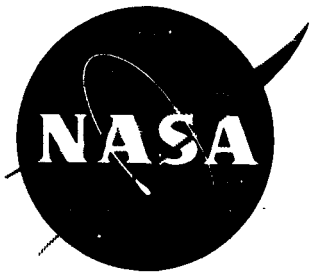

TECHNICAL MEMORANDUM

X-385

DESIGN CONCEPTS IN MILLION-POUND-THRUST-CLASS SPACE VEHICLES FOR REDUCTION OF OVERALL STRUCTURAL WEIGHT AND EVAPORATIVE LOSSES IN UPPER-STAGE CRYOGENIC PROPELLANTS

By Rinaldo J. Brun and Edmund G. Rosenberg

Lewis Research Center
Cleveland, Ohio

NATIONAL AERONAUTICS AND SPACE ADMINISTRATION
WASHINGTON
August 1960

NATIONAL AERONAUTICS AND SPACE ADMINISTRATION

TECHNICAL MEMORANDUM X-385

DESIGN CONCEPTS IN MILLION-POUND-THRUST-CLASS SPACE VEHICLES FOR REDUCTION OF OVERALL STRUCTURAL WEIGHT AND EVAPORATIVE LOSSES IN UPPER-STAGE CRYOGENIC PROPELLANTS*

By Rinaldo J. Brun and Edmund G. Rosenberg

SUMMARY

This report describes vehicle design concepts that exploit the latitude in stage arrangement and thrust transmission permitted by the large size of vehicles in the million-pound-or-more-thrust class. The two principal concepts introduced in this report are: (1) the telescoping of the second-stage cryogenic propellant tanks into the liquid-oxidant tank of the booster stage, and (2) the transfer of engine thrust forces through structural members acting in tension only. These concepts minimize the penalty of evaporative losses of cryogenic propellants on payload and reduce the structural weight of the vehicle.

Three versions of a space vehicle designed with a booster thrust of one million pounds each are presented in order to illustrate the utility of the design concepts. A hydrogen-oxygen propellant combination was assumed in all stages of the vehicles because this high-energy combination permits considerable payload for space missions. However, the basic principles of design discussed in this report also apply to other propellants.

The study also includes typical missions and payloads possible with the three illustrative large hydrogen-oxygen versions of a space vehicle. With conservatively assigned values of allowable stress in the material, as well as conservative weight estimates of the engines and accessories, a two-stage design will orbit a 42,000-pound net payload (net payload excludes the disposable weight of last stage) in a 300-nautical-mile circular orbit. A two-stage vehicle will provide escape capabilities for a 13,900-pound net payload. A three-stage vehicle provides escape capabilities for a 17,500-pound net payload. The total vehicle mass fractions range from 0.94 to 0.95. Less conservative designs, with consequent greater payloads, are also discussed in the report.

*Title, Unclassified.

INTRODUCTION

Many of the proposed missions for space exploration require large-thrust launching vehicles. Further, a considerable advantage in payload is gained when high-energy propellants are used, particularly in the upper stages. The use of liquid-hydrogen fuel in a hydrogen and oxygen propellant combination, however, presents large problems because of its low temperature and density. The transport of liquid hydrogen through the Earth's atmosphere involves an evaporative loss by virtue of the aerodynamic heating encountered. Insulation weights required in order to reduce this evaporative loss impose a serious payload penalty. Also, because the density of liquid hydrogen is extremely low, the large tanks required may be longer than those used for fuels of greater density, with consequent increase in the bending moments within the structure.

Since the problems associated with the use of liquid hydrogen as a high-energy propellant, such as structural weight and insulation, may limit its utility in multistage vehicles of conventional tandem stage arrangement, a study was made at the NASA Lewis Research Center of vehicle design configurations that minimize many of the disadvantages. This report describes such a vehicle design that exploits the latitude in stage arrangement permitted by the large size of vehicles in the million-pound-thrust class. The study suggests rather radical design techniques in an attempt to substantially reduce rocket booster weight. Similarities exist between some concepts presented herein and those proposed by Oberth as early as 1923 (refs. 1 and 2) although, perhaps, for different reasons. As a test of the utility of the concepts, three versions of a vehicle were evolved for use in mission studies. The computed performance of each vehicle is described. The expected loss of cryogenic propellants during ascent through the atmosphere is also presented.

The three versions of this vehicle employ liquid hydrogen for fuel in all the stages. The principal concepts of design apply equally well to vehicles fueled with hydrocarbons in the first stage and hydrogen in the upper stages. A detailed comparison among the many possible propellant combinations and different design concepts is not within the scope of this report. The specific vehicle evolved is intended only as an illustrative example in the application of concepts permitted with large-scale vehicles.

VEHICLE DESIGN

The two principal objectives of this design study are (1) to minimize the evaporative loss of cryogenic propellants in the upper stages and (2) to minimize the structural weight of the vehicle. These two objectives were fulfilled in part by the introduction to the large million-pound-class vehicles of new concepts in geometry and structural configuration that are not possible with small vehicles. For example, the

liquid-hydrogen and liquid-oxygen tanks of the second stage are immersed in the oxygen of the booster stage in order to protect the second-stage propellants from aerodynamic heating while passing through the atmosphere at high speed.

The approach to minimizing the structural weight of the vehicle was to eliminate the transfer of thrust force through structural members in compression wherever possible. This is accomplished by mounting the engine inside the bottom tank in order that part of the thrust may be resisted by fluid pressure in direct contact with the engine and the remainder may be transmitted as tension in the tank bottom membrane. These concepts are illustrated in greater detail in subsequent sections and are applied to three versions of a vehicle evolved to demonstrate the utility of these schemes. The vehicle was evolved to determine the orbital payload capabilities about 300 nautical miles above the Earth's surface and to determine the escape payload capabilities for a two-stage and a three-stage vehicle.

Second-Stage Immersion

The second stage is telescoped into the booster stage for structural reasons, as well as for reducing the evaporative losses. Figure 1 shows a version of a two-stage space vehicle with the second-stage propellants and engine buried in the oxygen tank of the booster stage.

The structural reasons for second-stage immersion become apparent when compared with a more conventional tandem design. When the second stage is placed on top of the booster in a tandem arrangement, the engine section of the second stage is tied to the upper tank of the booster by heavy structural members and/or a skirt. This transition section must carry large bending and acceleration loads during the booster firing time. Telescoping the second stage within the oxygen tank of the booster results in smaller bending loads in the booster tank because of shorter overall vehicle length for a given diameter due to the elimination of the transition section between the booster and second stage. Also, smaller bending loads occur in the second-stage structure during booster flight because the pure cantilever method of mounting is eliminated.

The minimum structural weight of the vehicles studied, with the second stage telescoped in the booster stage, was found to be a function of the length-to-diameter ratio of the overall vehicle. The optimum length-to-diameter ratio l/d was obtained by minimizing the gross takeoff weight required to accomplish a given mission. The values of l/d were varied from 2 to 8 while maintaining a nearly paraboloidal shape for the booster oxygen tank and a right circular cylinder for the hydrogen tank (fig. 1). For a pressure-stabilized-skin type construction, the overall structural weight of the vehicles designed to house a given volume of

fluid for a given mission decreases with increasing values of diameter, thus, with decreasing values of l/d. Because of bulkhead, geometry of multistaging, and limitations on thinness of tank wall material, structural weight savings became questionable below an l/d of about 2 for the designs studied.

When the aerodynamic drag was considered (as discussed in appendix A) along with the structural factors, the optimum value of l/d was greater than that due to structural weight alone. Below values of about $4\frac{1}{2}$, decreasing structural weight with decreasing values of l/d was more than compensated for by the increasing weight of propellants required to overcome the additional aerodynamic drag caused by the increasing cross-sectional area. Studies on three versions of the vehicle indicate that the minimum gross takeoff weight is insensitive to changing values of l/d near the optimum. For each of the versions studied, the curve was nearly flat for values of l/d between 4 and 6. Some latitude of compromise on the diameter is available to the designer if it is desired to standardize on one diameter value for several versions of a vehicle requiring some variation in the volume of the propellants for different missions. The value of 24 feet shown in subsequent figures of the vehicle studied was such a compromise.

The telescoping of the second stage within the booster is particularly important when cryogenic fluids are used as propellants. The high rate of fluid removal from the booster tanks (2940 lb propellant/sec for the illustrative examples studied herein) greatly diminishes the insulation problem on the booster stage after launching. The rate of gas formation at the tank walls due to heat input is not enough to maintain the required pressure in the tanks throughout the booster flight (although some gas must be released during a portion of the flight). (A discussion on heat input to the booster stage during the flight through the atmosphere is presented in appendix B.) A different problem is associated with the second stage because there is no fluid pumped from the tanks during that part of the flight through the atmosphere. If the second stage is directly exposed to aerodynamic heating by placing it in conventional tandem arrangement, a greater insulation problem results. Telescoping the second stage in the booster oxygen tank places the cryogenic fluids in a less hostile environment and reduces the required insulation to only a small amount around the hydrogen tank.

Engine Mounting and Thrust Transmission

The main reason for immersing the engine in the fuel tanks, as shown in figures 1 and 2, is to eliminate the transfer of thrust force through structural members in compression. The action of the force from the thrust chamber on the vehicle is very similar to that of pushing a finger

into a toy balloon. The principle of design applied here is to keep all the tank skins and large load-carrying members in tension. The tension in the skins is maintained by pressure in the tank. The tank pressure required to maintain the tension and the method of pressurizing are discussed later.

In the more conventional missile the pressure forces distributed inside the thrust chamber walls are collected on a ball joint, or its equivalent, and then transmitted through structural members in compression and shear to the tanks. The forces are again collected in a circumferential ring or skirt at the bottom of the tank and again redistributed through the tank walls and bottom.

In this proposal, shown in figures 1 and 2, the pressure forces inside the thrust chamber are partially balanced by the pressure forces inside the tank. The summation of the pressure forces directed axially upward inside the thrust chamber is greater than the summation of the tank pressure forces projected downward acting on the tank side of the thrust chamber walls plus the inertial force of the equipment mounted directly on top of the combustion chamber. The resulting difference between the sum of the inertia forces and the cumulative tank pressure force pushing down on the thrust chamber and the thrust force inside the chamber pushing up is carried as tension by the tank bottom membrane H attached to the thrust-chamber coolant manifold ring B (fig. 2). It is important to note two advantages here as compared to a conventional design. One advantage is that a significant portion of the engine thrust is immediately absorbed by the pressure force in the tank without transmission through structural members. The other advantage is that the remainder of the thrust is carried by a skin in tension rather than through columns in compression. These two advantages should result in a structural weight saving.

The shape of the tank bottom membrane H (fig. 2) is in the form of a half torus, obtained by the rotation of a semicircle of radius c about the centerline of the vehicle. The stresses introduced in the toroidal membrane when the tank is pressurized are derived in reference 3.

The question is raised as to whether the hot gases that will probably vortex out around the nozzle-exit rim at low altitudes and flare laterally at high altitudes might affect the tank bottom. This question of base heating cannot be answered without experimentation. In figure 2, the nozzle-exit rim is shown extended beyond the point of attachment of the bottom membrane H to the coolant manifold ring B. The extent to which the engine is projected through the missile bottom and the amount of baffling that can be used as a remedy for base heating must be determined experimentally. A further extension of the nozzle by twice as much as shown in figure 2 will not appreciably affect the advantages of the immersion mounting.

Engine Gimbaling

Vehicle steering is not simple but may be obtained by various methods such as auxiliary steering motors located either near the nose or around the bottom, jet vanes, unbalanced peripheral fluid injection in the nozzle, or engine gimbaling. Because of the trajectories assigned for the missions (appendix A), the magnitudes of wind gusts assumed encountered (see p. 8), and the relation of the center of pressure with respect to the center of gravity when the wind gusts are applied, engine gimbaling of $1\frac{1}{2}^{\circ}$ has been calculated as ample for the versions of the vehicle studied herein. With such small gimbaling requirements, the complete engine assembly, including the pressurized accessories room to be discussed in a subsequent section, can be gimbaled in any desired direction from the vehicle centerline.

The rings B, F, J, and K (fig. 2) and the members connecting the rings are an integral part of the gimbaling system. The gimbaling action can be applied through a number of hydraulic actuators L, which are supplied with high-pressure liquid hydrogen (800 lb/sq in. gage) bled from the fuel pump discharge. By proper operation of the actuators, the gimbaling creates a tipping of the manifold ring B about a centerline passing approximately through the point A. For a gimbaling action of $1\frac{1}{2}^{\circ}$, the maximum vertical displacement of two diametrically opposite points on the manifold ring is less than 3/4 inch from the neutral position, which is the position wherein the direction of the thrust vector passes through the vehicle center of gravity. This small displacement causes a very small change of radius of the membrane H; therefore, the membrane appears to remain well within the elastic limit at all localities. During gimbaling, the movement of the manifold ring B is in the direction of the mode of least restraint for the toroidal-shaped membrane H.

The frame and actuators also serve the purpose of preventing the rupture of the membrane H at the time of thrust cutoff when the tank pressure acts to force the engine assembly out through the tank bottom. A rupture of the membrane H may produce a nonaxial thrust caused by an unsymmetrical escape of the pressurizing gas from the tank. The action of an uncontrolled thrust before the clean separation of the second stage from the booster is undesirable. Coincident with burnout will be the unavailability of liquid hydrogen for the actuators L. With the unavailability of hydraulic fluid, the actuators will extend to the fullest length, and the load is carried through metal contact at the actuator piston stop.

The weight estimates given in appendix C for the frame and actuators are based on a frame designed with the capability of opposing a gas force of one million pounds acting on the manifold ring B (fig. 2). The weight estimates also include dampers M for minimizing oscillations of the engine assembly in a direction perpendicular to the vehicle centerline. These dampers must also operate with liquid hydrogen if mounted as shown in figure 2, but can be mounted with an insulated and heated dashpot

inside the accessories room, thereby making the use of other hydraulic fluids possible.

The method of engine mounting described in the preceding section can also be applied to a multiengine vehicle in which a center nongimbaling engine of very high thrust is surrounded by three or more small gimbaling engines. In this suggestion, the low-thrust gimbaling engines would transmit thrust in a conventional manner through a socket or universal joint; whereas, the high thrust from the central engine would be transmitted in the manner described, but with a solid connection FB replacing the actuator L (fig. 2).

Tank Pressures

In order to prevent buckling of the hydrogen and oxygen propellant tanks, the pressure in the tanks must be high enough to maintain the skin in tension under all axial and bending loads imposed on the vehicle. When only the axial load from the thrust chamber is considered, the minimum pressure in the hydrogen tank at the level of the ring J (fig. 2) required to support the tank walls and bottom membrane in tension is found from the expression

$$p_1 = \frac{F_t - W_t A_g}{\pi R_2^2} \tag{1}$$

where p_1 is the tank pressure in pounds per square inch gage required to prevent compressive stress in tank walls due to axial load only, F_t is the engine thrust in pounds, R_2 is the tank wall radius in inches, W_t is the sea-level weight in pounds of the complete engine, including the accessories and pump room directly attached to the thrust chamber, and $A_g = (F_t - D_a)/W$ where D_a is the aerodynamic drag in pounds and W is the vehicle weight in pounds at any instant. The product of A_g (known as pilot g's) and the weight of an object measured at sea level before thrust is applied will give the force on the object due to the action of the thrust chamber and drag. The components of force due to Earth gravity and centrifugal maneuvering must be added vectorially in order to obtain the total force supporting the object in the vehicle.

For the booster stage of the vehicle, shown in figure 1, the value of A_g varies from 1.5 immediately after firing to 6.4 immediately before burnout (appendix A). The value of W_t also varies slightly during the booster flight because the helium used in augmenting the tank pressurization has been assumed contained in the pump room. The variation in W_t caused by the helium consumption is too small to affect the value of p_1 significantly. The estimate for W_t is the sum of the thrust-chamber weight (5700 lb) and the auxiliary equipment (6840 lb) given in appendix C. The values of p_1 vary from 15 to 14.1 pounds per square inch gage from takeoff to burnout, respectively. To this gage

pressure must be added the pressure required in order to prevent buckling of the tank walls when the engine is gimbaled.

The tank pressure required to prevent buckling is obtained after the maximum bending moment is known. The angular acceleration of the vehicle is established as a function of altitude from the optimum trajectory for that vehicle. This trajectory is discussed in appendix A. The upsetting moments produced by wind shear and gusts are established from an assumed variation of wind velocity with altitude. For the problem studied herein, the wind velocity was assumed to vary approximately linearly from 80 feet per second at sea-level to 300 feet per second at a 35,000-foot altitude and then decrease to 150 feet per second at a 60,000-foot altitude. This severe wind speed variation appears to be a conservative design criterion.

A bending-moment diagram calculated for the most severe combination of required angular acceleration and wind upsetting moments is shown in figure 3 as a function of vehicle station for one of the three vehicle versions studied. As can be seen, the maximum bending moment is 690,000 pound-feet and occurs about 36 feet from the bottom. The bending moment introduces tension stresses in one side of the tank wall and compressive stresses in the diametrically opposite side. In order to avoid buckling on the compression side of the tank, the tank is pressurized to such an amount that the resulting longitudinal tensile stress due to pressure counteracts the compressive stress due to bending. This equality of tensile and compressive stresses is given by

$$s_t = \frac{p_2 R_2}{2t} = s_c = M \frac{c}{I} \tag{2}$$

which for a thin annulus reduces to

$$p_2 = 2M/\pi R_2^3 \tag{3}$$

where p_2 is the tank pressure in pounds per square inch gage required to prevent compressive stress in the tank walls due to bending only, s_t and s_c are the tensile and compressive stresses, respectively, in pounds per square inch, t is the wall thickness in inches, M is the bending moment in pound-inches, c is the distance in inches from the neutral axis to the extreme fibers under stress, and I is the cross-sectional moment of inertia in inches^4.

For the vehicle discussed herein the pressure p_2 is calculated to be slightly less than 2 pounds per square inch. In order to assure that the tank walls are always in tension, this value was arbitrarily raised to 4 pounds per square inch. Thus, the total pressure at the level of the ring J (fig. 2) required in order to prevent tank wall buckling is the pressure obtained from equation (1) plus the pressure selected in this paragraph, which totals 19 pounds per square inch gage. The tanks were designed for a pressure of 30 pounds per square inch gage, which is

the pressure assumed necessary at a short time preceding burnout because of pump cavitation requirements (see appendix B for hydrogen temperature variation with flight time).

The gas pressure at the top of the hydrogen tank is reduced from that at the level of the ring J by the hydrostatic pressure of the hydrogen liquid, with proper consideration for the vehicle acceleration; and the pressure at the bottom of the tank is increased by the hydrostatic hydrogen head.

At the beginning of flight, the pressure in the oxygen tank is 36 and 2 pounds per square inch gage at the bottom and at the top, respectively. Near burnout, a pressure of about 20 pounds per square inch gage again suffices for structural stability; however, the tank was designed for a pressure of 36 pounds per square inch gage in order to accommodate pump requirements near burnout. The second stage is supported by the fluid pressure in the oxygen tank, and, thus, the oxygen tank wall of the booster stage is not in axial compression.

The minimum pressure required in the second-stage tanks for structural stability during the second-stage firing is less than 19 pounds per square inch gage. In order to provide for possible pump cavitation requirements and to prevent collapse during booster flight, the second-stage tanks are designed for a pressure of 36 pounds per square inch gage.

Method of Pressurization

For the illustrative vehicle studied, the propellant tanks are assumed pressurized by a combination of self-pressurization and helium gas. As is discussed in appendix B, during a portion of the booster flight aerodynamic heating is sufficient to evaporate more hydrogen and oxygen than can be accommodated as gas in the respective tanks. No pressurizing helium is required during that portion of the flight when propellant gas is expelled overboard to prevent overpressurizing the tank. Helium augmentation was chosen in preference to a complete self-pressurization system because of the many uncertainties associated with the latter system. The weight estimates for the pressurizing system given in appendix C are based on a liquid-helium storage system.

Accessories Room

The turbopumps, heat exchangers, auxiliary power supply, gas generator, engine and pump controls, tank pressurizing equipment, and some other accessories are in the pressurized room mounted on top of the engine, as shown in figure 2. Two access tunnels are shown connecting the pump room with the outside skin of the hydrogen tank. Bellows in the

tunnels are necessary because during gimbaling the engine rotates about a center at A so that the pump room must move with respect to the tank walls. The turbopumps are placed on top of the thrust chamber to bolster the top of the thrust chamber structurally and to eliminate flexible high-pressure lines.

The turbopump rooms of the booster and the second stage are pressurized to the same pressure as the respective hydrogen tanks.

Intake Lines

The hydrogen intake lines to the pump are shown at C and the high-pressure lines from the pump to the thrust chamber are shown at D (fig. 2). The thrust-chamber coolant manifold ring B at the nozzle exit is fed by several high-pressure lines D. The oxygen intake line to the pump is shown at E. Bellows are necessary at each end of the intake line to allow for engine gimbaling. Insulation is placed around the pipe because it is immersed in liquid hydrogen.

Prelaunch Considerations

The vehicle must be supported on a stand while it is on the ground being loaded. The requirement in the design of the ground support stand is to find places on the vehicle where the supports will not stress any member of the vehicle more than that member is stressed during flight, if possible. In this manner, during flight the vehicle will not have to carry extra metal structure that is used only for ground support. During flight for the vehicle shown in figure 1 the resultant total force distributed around the tank bottom membrane H, where it is attached to the thrust-chamber coolant manifold ring B, is about 2/3 million pounds. This value of distributed force on the membrane is equal to the gross launching weight of the vehicle. Therefore, a good place to support the weight of the whole vehicle while on the ground would be on the exit rim of the exhaust nozzle. Except for the portion of the exhaust nozzle between the manifold ring and the rim, no other part of the vehicle is stressed while on the ground as much as it is designed to be stressed during flight.

Present experience in the launching of missiles indicates that long countdowns and holds are often required. The oxygen will freeze in the pipe between the oxygen tank and the pump room if the liquid in the pipe is not kept moving through the pipe during countdown and pumped with an external (ground) pump back into the oxygen tank. This recirculation eliminates additional pipe insulation required only during the countdown period and supercools the oxygen pumped back into the oxygen tank, at the

expense of the latent heat in the hydrogen. The recirculation places a small additional burden on the hydrogen tank topping.

During the countdown periods the hydrogen tank must be insulated, and it is desirable to insulate the complete vehicle. The insulation is stripped off at the time the booster is ignited because, during a large portion of the flight path, the volume rate at which the liquid propellants are pumped is greater than the volume rate at which gas is created by heat transfer through the tank walls. As is discussed in appendix B, some propellants, particularly oxygen, may have to be valved off during a portion of the booster flight if the tanks are not provided with insulation. The overall consequence on the payload of providing insulation appears to be more detrimental than expelling the excess gas. A brief study revealed that insulation that is carried to the end of the booster flight must weigh less than one-half the weight of gas valved off during the first 40 seconds of flight in order to have the same detrimental effect on payload.

MISSION CAPABILITIES

Three versions of the vehicle were evolved to demonstrate the utility of the foregoing schemes and thereby arrive at some mission capabilities for the proposed vehicle. One version was derived to determine the size of payload that could be placed in a circular orbit about 300 nautical miles above the Earth's surface. The two other versions were evolved to determine the payload that could escape from the Earth's gravitational field for use in outer-space studies. The two versions intended to demonstrate escape capabilities differ from each other in that one is a two-stage vehicle and the other has three stages. One-million-pound thrust was assumed on the booster, and hydrogen and oxygen were the propellant combination for all three versions of the vehicle.

A 200,000-pound-thrust engine was assumed for the second stage of all three versions. Other data and pertinent parameters are given along with the details of the weight estimates in appendix C.

Although an optimum trajectory is associated with each of the three proposed versions and missions, the trajectories calculated with electronic computing equipment accounted for a nearly optimum path for accomplishing each mission. More refined trajectories than those applied to the missions discussed will result in at least as much payload as reported. Some computed details of the trajectories are given in appendix A.

Two structural weight calculations have been made for each of the three proposed versions. One set of calculations conceives a design based on good fabrication practice available in industry at the present

time. This design takes advantage of known recent improvements in material strengths and fabrication procedures but does not impose unknown factors of future improvements in industry. This design permits the immediate fabrication of the vehicle with a minimum of development uncertainties. The weights computed on this conservative design philosophy will be referred to as "estimate A." The second set of structural weight calculations referred to as "estimate B" is based on a modest anticipated improvement in material strength and fabrication procedure in industry and on an improvement potential on this type of vehicle. Some details on the structural weight for both estimates are given in appendix C.

Two-Stage Orbiting Vehicle

The two-stage orbiting vehicle is shown in figure 4. Two sets of dimensions are shown in the figure. The dimensions labeled "orbit" apply to the orbiting vehicle discussed in this section; the dimensions labeled "escape" apply to the two-stage escape vehicle discussed in the next section.

The essential weights and mass fractions of the two-stage orbiting vehicle are given in the following table:

		Estimate A		Estimate B	
		Weight, lb	Mass fraction	Weight, lb	Mass fraction
Total vehicle	Disposable Propellant	36,450 588,600	0.942	30,050 591,400	0.953
Booster	Disposable Propellant	25,800 485,100	0.952	21,500 485,100	0.959
Second stage	Disposable Propellant	10,650 103,500	0.912	8,550 106,300	0.929
Payload plus guidance		41,950		45,700	

The disposable weight is the combined weight of tanks, engine, frames, and unused propellants that are discarded as part of the stage being separated from the remainder of the upper stages. A more detailed weight distribution is given in appendix C, and a description of the trajectory is presented in appendix A. The guidance intelligence system was included as part of the payload because a major portion of the intelligence equipment that is used in guiding the vehicle into orbit might be used in determining the location of the payload while orbiting and returning to the Earth's surface.

The mass fraction is defined as:

$$\frac{\text{Useful propellants}}{\text{Disposable weight + Useful propellants}}$$

In a multistage vehicle the mass fraction is a measure of the effectiveness of structural design of each stage, or of the overall vehicle, without including the payload. Mass fraction is a simple index of effectiveness in comparing the design of stages in a multistage vehicle, as well as among vehicles. It should be noted that mass fraction differs from the usual definition of mass ratio in that mass ratio is usually defined as the ratio of effective propellant mass to initial vehicle mass. The payload is included in the initial vehicle mass. A vehicle with large payload, high-specific-impulse propellants, and low disposable weight would reflect a low mass ratio when compared with a vehicle with smaller payload, lower specific impulse propellants, and comparable disposable weight, although the mass fractions could be the same.

Although some consideration was given to a three-stage orbiting vehicle, the three-stage version is not treated herein because the small added payload (about 10 percent) is considerably offset by the added complexity and by the reduced reliability of the added staging.

Two-Stage Space Vehicle

The dimensions for a two-stage space vehicle are also shown in figure 4. As used herein, the term space vehicle means that the payload has attained sufficient velocity and altitude to escape from the Earth's gravitational field. The mission beyond the attainment of escape velocity is not treated here. The essential weights and mass fractions are given in the following table:

		Estimate A		Estimate B	
		Weight, lb	Mass fraction	Weight, lb	Mass fraction
Total vehicle	Disposable Propellant	36,050 617,050	0.948	30,000 618,300	0.954
Booster	Disposable Propellant	25,200 499,800	0.951	21,400 499,800	0.956
Second stage	Disposable Propellant	10,850 117,250	0.920	8,600 118,500	0.936
Payload plus guidance		13,900		18,800	

A more detailed weight distribution is given in appendix C, and trajectory data are presented in appendix A.

Three-Stage Space Vehicle

A three-stage space vehicle is shown in figure 5. The principal advantage of the three-stage vehicle over the two-stage version is the increase in escape payload. The two principal disadvantages are (1) additional unreliability with introduction of additional complicated working parts in the whole system, and (2) the development of an additional engine. The second disadvantage is not serious because, if the emphasis is placed on soft landings on the Moon, the engine used in the third stage of the space vehicle can also be used for landings on the lunar explorations. The essential weights and mass fractions are given in the following table:

		Estimate A		Estimate B	
		Weight, lb	Mass fraction	Weight, lb	Mass fraction
Total vehicle	Disposable	40,390	0.938	33,500	0.950
	Propellant	609,150		614,700	
Booster	[a]Disposable	25,950	[a]0.944	21,500	[a]0.953
	Propellant	426,300		426,300	
Second stage	Disposable	11,440	0.938	9,200	0.950
	Propellant	157,150		161,050	
Third stage	Disposable	3,000	0.873	2,800	0.906
	Propellant	25,700		27,350	
Payload plus guidance		17,500		19,400	

[a]Includes weight of third-stage insulation, which is discarded at time of booster discard.

Since the third-stage engine is small physically and, in addition, has low thrust (40,000 lb, see appendix C), the method of mounting is not critical. This engine can either be buried or mounted conventionally, depending on which geometry can be best adapted to the payload and overall vehicle geometry. As shown in figure 5, the engine is pushing directly on the payload rather than through the tanks. The propellant tanks surround the engine, with the oxygen tank surrounding the hydrogen tank. Although this geometry of tank design does not produce the lowest tank surface to volume ratio, it was chosen in order to eliminate a heavy

weight transition section. The problem of insulation between the hydrogen and the atmosphere is reduced by surrounding the hydrogen with oxygen.

Two concepts were studied regarding the protection of the third-stage cryogenic propellants from dynamic heat while the vehicle is proceeding through the atmosphere. In one concept, the third stage was telescoped into the oxygen tank of the second stage in the same manner as the second stage was telescoped into the oxygen tank of the booster. In the other concept, shown in figure 5, the third stage was conservatively protected with a 2-inch layer of laminated fibrous asbestos insulation surrounded with stainless steel foil. The weight comparison of the two concepts shows a considerable advantage with the insulated third-stage design concept for two main reasons. The total weight of the telescoped design is about 1300 pounds greater than that of the insulated third-stage design because the surface-to-volume ratio of the booster oxygen tank increases considerably. This increase in surface increases the weight of the oxygen tank and, more important, increases the heat input to the liquid oxygen, thus requiring a greater expulsion of oxygen gas in order to prevent bursting of the tank during booster flight. The telescoping of the third stage into the second stage may be advantageous for vehicles larger than those studied here. The payload weights shown in the preceding table assume that the insulation and external protective foil are discarded with the booster.

CONCLUDING REMARKS

This study was made to determine a value for mass fraction that reflects the use of rather radical design concepts. Although there may be some uncertainty as to the reliability of some of the concepts introduced because no experimentation was employed in support of the ideas, the report is intended to give designers of very large boosters a different look at booster design study than is common practice with smaller vehicles. Some savings in weight appear possible with these concepts, but this is not a proven fact because no comparison was made with a conventional design of the same thrust level. Furthermore, because detailed designs were not attempted for this presentation, the configurations evolved herein are not recommended as final vehicles without further refinements in the analyses for the engine mounting and second-stage support.

SUMMARY OF RESULTS

The two principal concepts introduced in this report are: (1) telescoping of the second-stage cryogenic tanks into the liquid-oxygen tank of the booster stage, and (2) the elimination of the transfer of engine

thrust force through structural members in compression wherever possible. As a result of the first concept, the evaporative losses of cryogenic propellants used in the second stage are minimized. The overall structural weight of the vehicle is reduced for the following reasons:

1. With second-stage immersion the upper stages and payload are supported by gas pressure rather than structural members in compression.

2. As compared with a tandem arrangement, smaller bending loads result in both the booster tanks and in the second-stage structure.

3. With the second stage telescoped into the booster oxygen tank the insulation problem is eased, both as to amount of insulation and amount of covering protecting the insulation against aerodynamic loads.

4. With the engine immersed in the fuel tank a large portion of the thrust load (about one-third for the versions of the vehicle studied) is absorbed by the pressure force in the tank and the weight of the pumps and accessories placed directly on the thrust chamber, without transmission through structural members. The remainder of the thrust is carried by the tank bottom membrane in tension.

Vehicles evolved to test the utility of the proposed design concepts resulted in overall vehicle mass fractions ranging from 0.94 to 0.95, with hydrogen and oxygen as propellants in all the stages. With conservatively assigned values of allowable stress in the material, as well as conservative weight estimates of the engines and accessories, a two-stage design will orbit a 42,000-pound net payload (with guidance) in a 300-nautical-mile circular orbit. A two-stage vehicle will provide escape capabilities for a 13,900-pound net payload. A three-stage vehicle provides escape capabilities for a 17,500-pound net payload.

Lewis Research Center
National Aeronautics and Space Administration
Cleveland, Ohio, February 15, 1960

APPENDIX A

TRAJECTORIES OF VEHICLES

An optimum trajectory is associated with each of the three proposed versions of the vehicle and the missions. The design of each version is in turn related to the trajectory because the number of stages and the apportioning of the propellants among the stages are related to the mission and the trajectory. The optimization of the staging and trajectory is an iteration process. The trajectory and staging of the three versions studied were optimized at least to a degree compatible with the uncertainty in the design weights. Also, the uncertainties in the trajectories and staging are such that further refinement will result in at least as much payload as reported herein.

The staging optimization is based on the principle that the amount of useful work assigned to each stage is proportional to the effectiveness of the stage. The term "useful work" means work done on the payload. Although the first stage performs a large amount of total work in lifting and accelerating the whole structure and most of the propellants, it does only a small fraction of the useful work on the payload. Because the specific impulse of the second stage is 410 seconds as compared with 340 seconds in the first stage, the second stage was assigned a proportionately greater amount of useful work to be done on the payload than the first stage, and the quantities of propellants were assigned accordingly. Besides the specific impulse, other factors governing the staging were: aerodynamic drag resulting in a reduction of booster effectiveness, ratio of structural to total weight in each stage, and steepness of trajectory during the burning period. A trajectory that requires lifting large quantities of propellants against the force of gravity results in a stage with low effectiveness.

The question of the proper value for coefficient of drag C_D during the booster portion of the trajectory was investigated to a limited extent. Changing the values of C_D by 30 percent from 0.4 was found to have negligible effect on the payload performance. The trajectory values given in tables I to III are for an average value of C_D of 0.4.

The tabulations in tables I to III are values of the nearly optimum trajectories and attendant velocities and gross weight for the three versions of the vehicle studied. The original calculations were made with digital electronic computing equipment at 10-second intervals, but are tabulated here at 20- and 40-second intervals for brevity. A rotating spherical Earth is assumed. The range, in nautical miles, is the horizontal (circular) distance from the radius passing through the launching pad. The velocity is relative to the center of the Earth.

The velocity at zero second given in each of the three tables is the peripheral velocity of the Earth at a latitude corresponding to Cape Canaveral, Florida, U.S.A. (approx. 28^{o}). The altitude is measured from sea level.

For the orbiting vehicle the million-pound-thrust booster stage burns for 165 seconds. During this burning time the vehicle maneuvers so that at booster burnout the velocity vector is at an angle of 9.06^{o} with respect to the local horizontal. The booster burnout takes place at an altitude of 191,289 feet (31.4 naut. miles). (Values of altitude in ft are obtained from computing machines, and the significant figures reported do not denote the accuracy required for performing the mission.) The velocity with respect to the Earth's surface is 11,186 feet per second, and the acceleration is about 5.9 pilot g's, which is the largest value encountered during the complete orbiting mission. (For definition of pilot g's, see section entitled "Tank Pressures" in text.)

After the booster separation the second stage ignites and burns for 208 seconds with a thrust of 200,000 pounds to an altitude of 42.8 nautical miles. The 208-second burning time is followed by a coasting period during which the altitude increases from 42.8 to 300 nautical miles. At the end of the coasting period the absolute velocity is 24,260 feet per second, which is below the absolute velocity required for orbiting; therefore, the coasting period is followed by an impulse of 776,000 pound-seconds, which is equivalent to a burst of 3.88 seconds of full thrust from the second-stage engine.

For the two-stage escape version of the vehicle, the million-pound-thrust booster stage burns for 170 seconds to an altitude of 200,298 feet (32.9 naut. miles). The velocity vector has an angle of 8.5^{o} with respect to the local horizontal, and the burnout velocity of the booster with respect to the Earth's surface is 12,167 feet per second, with a maximum of 6.4 pilot g's. After the booster separation the second stage ignites and burns for 241 seconds with a thrust of 200,000 pounds.

Second-stage burnout occurs at an altitude of 268,700 feet (44.3 naut. miles). The absolute burnout velocity with respect to the center of the Earth is 36,400 feet per second, and a maximum of 8.2 pilot g's is encountered during the mission.

For the three-stage version of the space vehicle, the million-pound-thrust booster stage burns for 145 seconds to an altitude of 221,255 feet (36.3 naut. miles). The velocity vector is 7685 feet per second (with respect to the Earth's surface) at an angle of 26.9^{o} with respect to the local horizontal, with an attendant 4.5 pilot g's. After the booster separation the second stage ignites and burns for 322 seconds with a thrust of 200,000 pounds. Burnout of the second stage takes place at an altitude of 464,729 feet (76 naut. miles), with a maximum of 3.5

pilot g's. After separation of the second stage, the third stage is ignited and burns for 263 seconds with a thrust of 40,000 pounds to an escape velocity of 36,500 feet per second, with a maximum of 2.0 pilot g's.

The trajectory values of altitude, velocity, and acceleration (pilot g's) given anywhere in this report (including tables I to III) apply only to versions of the vehicle described as estimate A in appendix C. The optimum trajectory for each model termed estimate B of a given vehicle changes. In fact, an optimum trajectory is associated with each change in design. Although detailed results are not presented in this report for the versions of each vehicle termed estimate B, optimum trajectories were calculated in order to obtain the values given for payload in appendix C.

APPENDIX B

HEAT INPUT TO BOOSTER TANKS

Calculations were made with a digital computer to determine the heat input to the hydrogen and oxygen tanks of the booster stage. The objectives of the calculations were to determine if the temperature of the tank walls above the liquid level exceeded the permissible safe operating values and to determine the quantities, if any, of hydrogen and oxygen lost through a pressure relief valve in order to prevent bursting of the tanks. Another important answer resulting from the calculations is the temperature of the last portions of liquid hydrogen and oxygen pumped from the tanks. This temperature is important for the cavitation factor in the turbopump design.

The results presented in this section are for the three-stage escape vehicle shown in figure 5. The geometric design of this vehicle results in a slightly greater heat influx than the other two vehicles studied.

The temperature immediately outside the boundary layer, that is, the temperature driving the heat into the tanks, was calculated from the flight Mach number and ambient atmospheric temperature using equations developed in reference 4. The values of Mach number and altitude were obtained from the trajectory calculations discussed in appendix A. The boundary-layer heat-transfer coefficient was determined as a function of surface distance from the nose of the vehicle by the method discussed in reference 5. No attempt was made to evaluate the effect of liquefaction of air on the hydrogen tank. If the oxygen and nitrogen in the atmosphere condense on the hydrogen tank during flight, the values of heat input discussed in this appendix may be changed considerably. The total heat input to each tank is divided into three parts: (1) heat into the tank wall and gas located above the liquid level, (2) heat that evaporates liquid in contact with the tank walls, and (3) heat that raises the bulk temperature of the liquid.

The temperatures of the tank walls at a station midway between the liquid level and the top bulkhead of the tanks are shown in figures 6(a) and (b) for the hydrogen and oxygen tanks, respectively. The midway station changes as the liquid level drops during the time of flight. The temperatures shown in figure 6 are pessimistic because all the heat has been assumed retained in the 0.030-inch-thick stainless steel tank walls; that is, none of the heat driven into the walls has been assumed transferred to the gas in the tanks. The results of similar temperature calculations are shown in figure 7 for the 0.012-inch-thick stainless steel skin covering the insulation on the third stage located on top of the oxygen tank. As with the tank walls, the calculations were simplified

to the extent that none of the heat driven into the skin was assumed transferred to the insulation making inside contact with the skin. Because of this assumption and because the third stage is located where the aerodynamic heating is greater than further aft, the highest calculated temperature of 730° Rankine shown in figure 7 is the highest temperature that can be expected at any station in the tank walls. Further refinements in the calculations are not necessary because the values shown in figure 7 are below the permissible operating temperatures consistent with the allowable stress assigned to the material used for the weight estimates.

The heat flowing into the tank below the liquid level was computed using the method reported in reference 5. The method recognized that film boiling might occur at the inner wall. In the calculations at each step that the heat flux through the tank walls was computed, the program first tested by a simplified method whether film boiling was occurring. If film boiling was indicated not to occur, the heat flux was calculated on the basis of liquid against the inner tank wall. If, however, the heat flow rate calculated by the simplified method was sufficient to support film boiling, the heat flow rate was recalculated to include the thermal resistance at the wall associated with the interior heat-transfer coefficient obtained from film boiling experiments reported in reference 5.

For presentation here, the heat into the tank below the liquid level is divided into that part which evaporates liquid in contact with the walls and that which raises the liquid bulk temperature. The proportioning ratio is not easily determined because of the many unknowns in the tank, such as convention currents and amount of temperature stratification. Two sets of calculations were made. For one set of calculations, all the uncertainties were assumed to be accumulative in the production of vapor at the tank walls. For the other set, the uncertainties were arranged to produce a minimum of evaporation and, thus, a maximum in the bulk temperature rise. The quantities of hydrogen evaporated within the maximum and minimum limits of uncertainties are shown in figure 8. During the vehicle booster flight the values of hydrogen evaporated are somewhere between the dashed and solid lines.

The result important to the operation of the vehicle is whether hydrogen must be valved off in order to prevent tank rupture. Gas valve-off is required if the rate of generation of gas volume is greater than the rate at which the volume of liquid is pumped from the tank. The rate at which excess hydrogen gas must be valved off is shown in figure 9.

The dashed line in figure 9 corresponds to the amount of hydrogen evaporated shown by the dashed line of figure 8. In order to require the valving of hydrogen, the cumulative formation of hydrogen vapor must be greater than that shown by the solid line of figure 8. In obtaining the results of figure 9, no hydrogen condensation on the liquid surface was

assumed. As given in figure 9, under the assumed extreme conditions represented by the area under the dashed line, approximately 1000 pounds of hydrogen must be expelled during the 60-second interval between 20 and 80 seconds after launching. When hydrogen is not being expelled, helium gas is furnished in order to maintain the design tank pressure.

The possible limits of oxygen gas valve-off from the oxygen tank are given in figure 10. Oxygen must be expelled from the oxygen tank even when the lower limit of heat input to evaporation is assumed (solid line). The reasons that the rates of oxygen vaporization are greater than for hydrogen are related to the differences in latent heat of the two liquids as well as to the greater surface of the oxygen tank. The quantity of oxygen valved off is about 1300 pounds under the solid line and approximately 2630 pounds under the dashed line.

The 2200-pound estimate for the weight of the pressurization system given in estimate A of appendix C assumed a most probable combination of helium required and hydrogen and oxygen valve-off in order to maintain the design tank pressure. The weight of the most probable combination is assumed to be about midway between the upper and lower values obtained from the curves of figures 9 and 10. The weight estimate includes the hydrogen and oxygen valved off together with the added helium. This pressurization weight estimate does not include the weight of propellants that remain as gas in the tanks at the time of booster burnout. This latter quantity is part of the 3200-pound unused propellant estimate (appendix C), which also includes the liquid in the pumps, lines, and thrust-chamber jacket.

The turbopump designer is interested in learning the temperature of the last portion of liquid that must be pumped in order to evaluate the factors involved in pump cavitation. The average temperature rise of the hydrogen liquid bulk as a function of time is shown in figure 11(a). The solid line is the counterpart of the solid line shown in figure 8; that is, the average bulk temperature is greater when the lower limit of evaporation at the walls is assumed. No temperature stratification was assumed in the liquid bulk. The temperature rise of the bulk liquid oxygen as a function of flight time is given in figure 11(b).

APPENDIX C

WEIGHT ESTIMATES

As has been stated in the section entitled MISSION CAPABILITIES, two structural designs have been made for each of the three vehicles. The designs, referred to as estimate A and estimate B, represent two degrees of conservatism in design. In most instances an itemized weight estimate for each of the two designs is given in this appendix. On some small items the difference is too small to report. On a few complicated items the difference is too involved to determine precisely; and, in these cases, the estimate is influenced by the more conservative design. The main source of difference in weight between the two designs is in the allowable stress and permissible minimum thickness. Estimate A was based on a maximum allowable stress of 150,000 pounds per square inch and a minimum tank wall and other large sheet thicknesses of 0.030 inch. Estimate B was based on a maximum stress of 200,000 pounds per square inch with a minimum permissible thickness on large sheets of 0.020 inch. The use of thinner material imposes greater difficulties in handling, welding, fabricating, and inspecting of material.

The specific impulse of the booster stage is assumed to be 340 pounds thrust per pound per second of propellant flow for all versions of vehicles. Optimum nozzle expansion was assumed to occur at a 10,000-foot altitude. The specific impulse was programmed into the trajectory calculations and varied slightly with altitude. A specific impulse of 410 seconds was assumed for the second and third stages. Other pertinent parameters are as follows:

Parameters	First stage	Second stage	Third stage
Thrust, lb	[a]1,000,000	200,000	40,000
Ratio of oxygen to hydrogen	5	5	5
Combustion-chamber pressure, lb/sq in. abs	600	350	350
Expansion ratio	7.8	33	35
Average value of ratio of specific heats in nozzle	1.22	1.22	1.22
Mean molecular weight of products	12	12	12
Flow rate through engine, lb/sec	2,940	488	97.6
Specific impulse	[a]340	410	410

[a]At 10,000-ft altitude.

Thrust Chamber

The thrust-chamber weight estimate is based on a channel construction for the walls, in which the hydrogen liquid enters the channels from the coolant manifold ring and leaves the channels at the combustion-chamber end of the thrust chamber. The inside and outside liners of the thrust chamber are designed to withstand a fluid pressure of 800 pounds per square inch gage for the million-pound-thrust chamber in the first stage and 500 pounds per square inch for the 200,000-pound-thrust chamber used in the second stage. The channel partitions are limited to a minimum of 0.020 inch in thickness for the conservative design in order to permit ease in fabrication and welding, although thinner material is permissible from a stress consideration. Material as thin as 0.010 inch is assumed possible in estimate B. Both estimates considered a possible 10-percent momentary overshoot in thrust output.

In the following table of weights for the thrust chamber are listed the weights of the principal members composing the thrust chamber. The plate at the head of the combustion chamber on which the injection nozzles are attached is listed as the nozzle plate. The head plate support acts as part of the structure for mounting the turbopumps in the pump room (see fig. 2). Between the nozzle plate and the head plate is a system of channeling separating the oxidant from the fuel and, also, acting as structural support between the nozzle plate and the head plate.

Thrust-chamber components	Weight, lb			
	Million-pound thrust		200,000-Pound thrust	
	Estimate A	Estimate B	Estimate A	Estimate B
Outside liner	1520	1430	600	580
Inside liner	1310	1240	540	510
Channeling between liners	370	230	110	80
Nozzle plate	310	260	90	70
Head plate	590	470	120	120
Channeling between plates	300	210	45	40
Coolant manifold ring	190	150	85	70
Hoops and stiffeners	300	250	65	30
Flanges, bolts, welding	500	400	45	30
Total	5390	4640	1700	1530

A breakdown weight estimate is not given here for the 40,000-pound-thrust chamber used in the three-stage vehicle because the weight for this thrust chamber is based on an existing experimental 20,000-pound-thrust chamber. The weight for the 40,000-pound-thrust chamber is estimated to be 300 and 250 pounds for estimates A and B, respectively.

Engine Auxiliaries

The equipment listed in the following table, like the thrust chambers of the previous section, is common to the three vehicles discussed herein. The turbopump weight includes the hydrogen pump, oxygen pump, turbine, gears, pump mounts, gas generator, and lubricating system. Pressurization includes the liquid helium and tanks, as well as hydrogen and oxygen valved off during flight. Controls include engine controls, hydraulic actuators, pressure controls, and starting system. The piping includes the ground fill and drain, pump inlets and outlets, piping to controls and heat exchangers, and so forth. Insulation is only the insulation used in the pump room, such as around the liquid-helium tanks and turbine exhaust pipe. The term frame means the frame surrounding the thrust chamber, used principally to orient the engine with respect to the centerline and to establish the center of rotation when the engine is gimbaled.

Components	Weight, lb			
	Million-pound thrust		200,000-Pound thrust	
	Estimate A	Estimate B	Estimate A	Estimate B
Turbopumps	1900	1700	330	300
Pressurization	2200	2000	900	850
Controls	400	340	180	160
Heat exchangers	210	130	80	70
Pump room	600	420	400	250
Piping	450	400	100	90
Electric wiring	110	100	60	60
Insulation	90	70	50	40
Frame	1500	1200	700	600
Total	7460	6360	2800	2420

The auxiliary components required in the third stage of the three-stage vehicle have been estimated to weigh about 300 pounds for both estimates A and B.

Tanks and Propellants

Because the propellant quantity is varied among the three vehicles in order to optimize the staging, the tank weights are not common to the three vehicles. The tank weights listed in the following table include the bulkheads, insulation, separation equipment, and stage support brackets, as well as welded overlaps and other miscellaneous items.

Item	Stage	Vehicle					
		Three-stage escape		Two-stage escape		Two-stage orbiting	
		Estimate A	Estimate B	Estimate A	Estimate B	Estimate A	Estimate B
Tank	1	[a]9,900	[a]8,100	9,150	8,000	9,750	8,100
	2	5,590	4,000	5,000	3,400	4,800	3,300
	3	1,950	1,850	-----	-----	-----	-----
Unused propellant	1	3,200	2,400	3,200	2,400	3,200	2,400
	2	1,350	1,250	1,350	1,250	1,350	1,300
	3	450	400	-----	-----	-----	-----
Total disposable weight	1	25,950	21,500	25,200	21,400	25,800	21,500
	2	11,440	9,200	10,850	8,600	10,650	8,550
	3	3,000	2,800	------	------	------	------
Propellant consumed	1	426,300	426,300	499,800	499,800	485,100	485,100
	2	157,150	161,050	117,250	118,500	103,500	106,300
	3	25,700	27,350	-------	-------	-------	-------
Payload plus guidance		17,500	19,400	13,900	18,800	41,950	45,700

[a]Includes weight of third-stage insulation, which is discarded at time of booster discard.

General Remarks

Both weight estimates given in this appendix and in the main text have taken into account a large extent of reliability in the engines and accessories. Although the overall structural concept is very different from conventional practice, it is felt that the weight estimates for the concept are quite conservative. It is anticipated that the vehicle discussed in this report will be used mainly for scientific studies of space. Only a few of these vehicles will be fabricated, thus obviating complicated and expensive jigs and fixtures associated with mass production. These same jigs and fixtures would aid in the fabrication of lightweight components. Economics dictate a compromise philosophy of design between absolute minimum structural weight, with the attendant expense, and ease of design and fabrication, with its attendant payload reduction for a given booster thrust level. The economics for a given mission and value of payload favor increasing the booster thrust and accepting less stringent structural weight requirements.

REFERENCES

1. Oberth, H.: Die Rakete zu den Planetenraümen. R. Oldenburg, Munich, 1923.

2. Oberth, H.: Wege zur Raumschiffahrt. R. Oldenburg, Munich, 1929.

3. Timoshenko, S.: Theory of Plates and Shells. McGraw-Hill Book Co., Inc., 1959.

4. Eckert, E. R. G.: Engineering Relations for Heat Transfer and Friction in High-Velocity and Turbulent Boundary Layer over Surfaces with Constant Pressure and Temperature. Trans. ASME, vol. 78, no. 6, Aug. 1956, pp. 1273-1283.

5. Kramer, John L., Lowell, Herman H., and Roudebush, William H.: Numerical Computations of Aerodynamic Heating of Liquid Propellants. NASA TN D-273, 1960.

TABLE I. - TRAJECTORY VALUES FOR TWO-STAGE ORBITING VEHICLE

Time, sec	Altitude, ft	Range, naut. miles	Velocity,[a] ft/sec	Mach number	Gross weight, lb
0	0	0	1,350	0	667,000
20	3,140	0	1,423	.3	608,200
40	13,458	0	1,769	.7	549,400
60	31,287	2	2,429	1.3	490,600
80	55,356	6	3,388	2.2	431,800
100	83,947	14	4,705	3.5	373,000
120	115,418	27	6,439	5.0	314,200
140	148,457	47	8,689	6.7	255,400
160	182,547	82	11,643	9.8	196,600
165	191,289	83	12,533	10.6	181,900
Second-stage ignition					
165	191,289	83	12,533		156,100
205	248,019	160	14,158		136,580
245	279,335	250	16,122		117,060
285	288,984	353	18,504		97,540
325	281,905	473	21,454		78,020
365	264,953	616	25,270		58,500
373	260,776	647	26,186		54,596
Coasting period followed by 3.88-sec burning time					
	1,822,830		24,820		52,600

[a]Absolute velocity with respect to Earth's center.

TABLE II. - TRAJECTORY VALUES FOR TWO-STAGE ESCAPE VEHICLE

Time, sec	Altitude, ft	Range, naut. miles	Velocity,[a] ft/sec	Mach number	Gross weight, lb
0	0	0	1,350	0	667,000
20	3,139	0	1,423	.1	608,200
40	13,458	0	1,769	.7	549,400
60	31,287	2	2,429	1.3	490,600
80	55,356	6	3,388	2.3	431,800
100	83,947	14	4,705	3.5	373,000
120	115,418	27	6,439	5.0	314,200
140	148,457	46	8,689	6.7	255,400
150	165,358	59	10,060	7.9	226,000
160	182,545	75	11,643	9.6	196,600
170	200,176	93	13,516	11.7	167,200
Second-stage ignition					
170	200,176	93	13,516		142,000
210	259,070	177	15,337		122,480
250	292,364	275	17,562		102,960
290	302,352	388	20,317		83,440
330	293,791	522	23,843		63,920
370	276,080	682	28,070		44,400
410	268,611	882	36,322		[illegible]
410.27	268,976	884	36,400		24,750

[a]Absolute velocity with respect to Earth's center.

TABLE III. - TRAJECTORY VALUES FOR THREE-STAGE ESCAPE VEHICLE

Time, sec	Altitude, ft	Range, naut. miles	Velocity,[a] ft/sec	Mach number	Gross weight, lb
0	0	0	1,350	0	667,000
20	3,141	0	1,414	.3	608,200
40	13,566	0	1,710	.7	549,400
60	32,307	1	2,291	1.3	490,600
80	59,862	5	3,178	2.2	431,800
100	97,037	11	4,439	3.3	373,000
120	144,778	22	6,117	4.5	314,200
140	204,987	39	8,286	6.9	255,400
145	221,255	44	8,923	7.7	240,700
Second-stage ignition					
145	221,255	44	8,923		214,750
185	348,523	92	9,750		195,230
225	450,516	147	10,831		175,710
265	525,384	211	12,183		156,190
305	571,539	285	13,834		136,670
345	588,010	371	15,833		117,150
385	574,842	471	18,260		97,630
425	533,631	588	21,266		78,110
465	468,408	727	25,146		58,590
467	468,500	735	25,372		57,614
Third-stage ignition					
467	468,500	735	25,372		46,179
507	468,510	893	26,629		42,275
547	468,515	1061	27,995		38,371
587	468,520	1238	29,490		34,467
627	468,520	1426	31,138		30,563
667	468,525	1627	32,980		26,659
707	468,580	1840	35,072		22,755
730	470,220	1973	36,250		20,500

[a]Absolute velocity with respect to Earth's center.

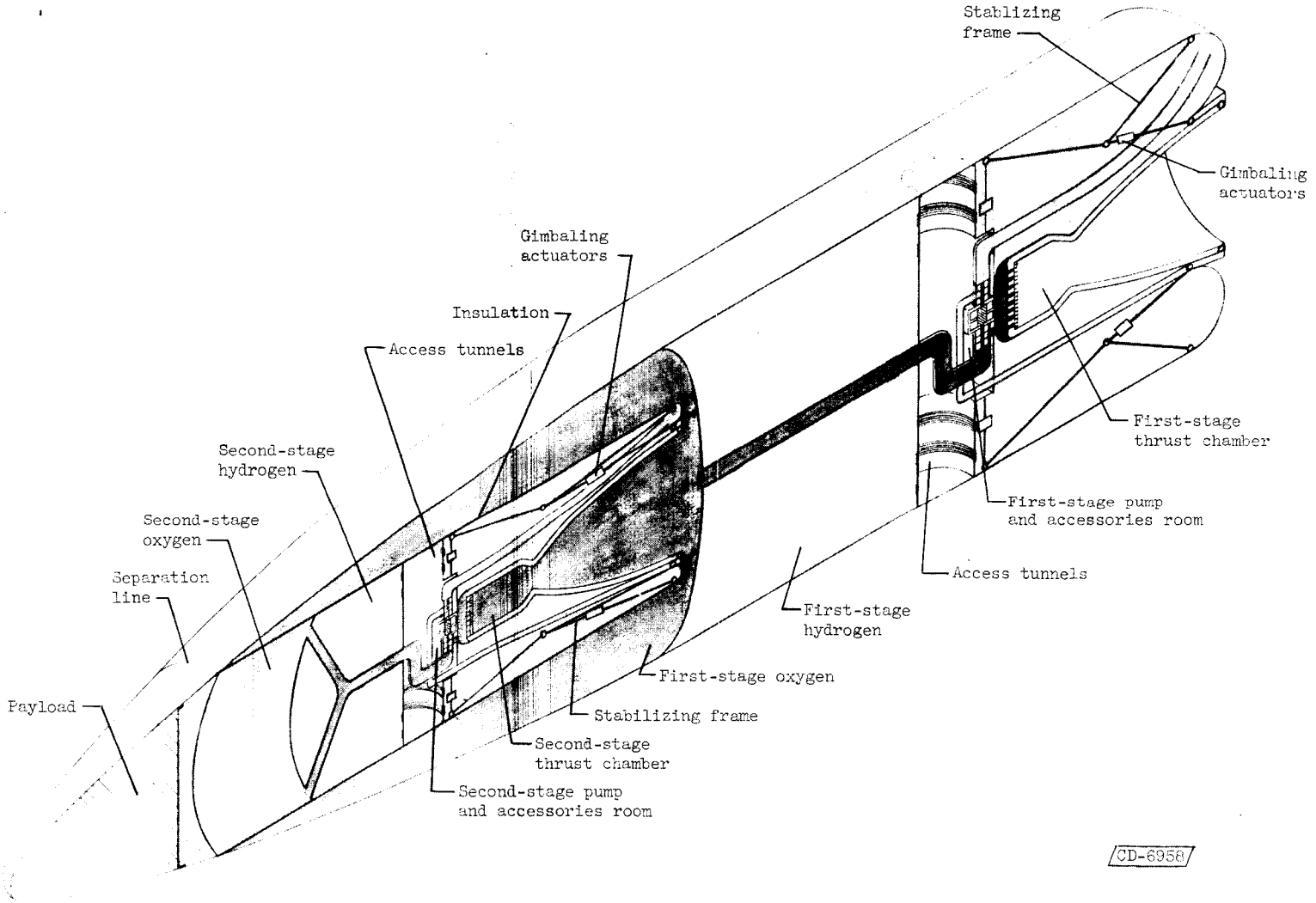

Figure 1. - Two-stage hydrogen-oxygen vehicle.

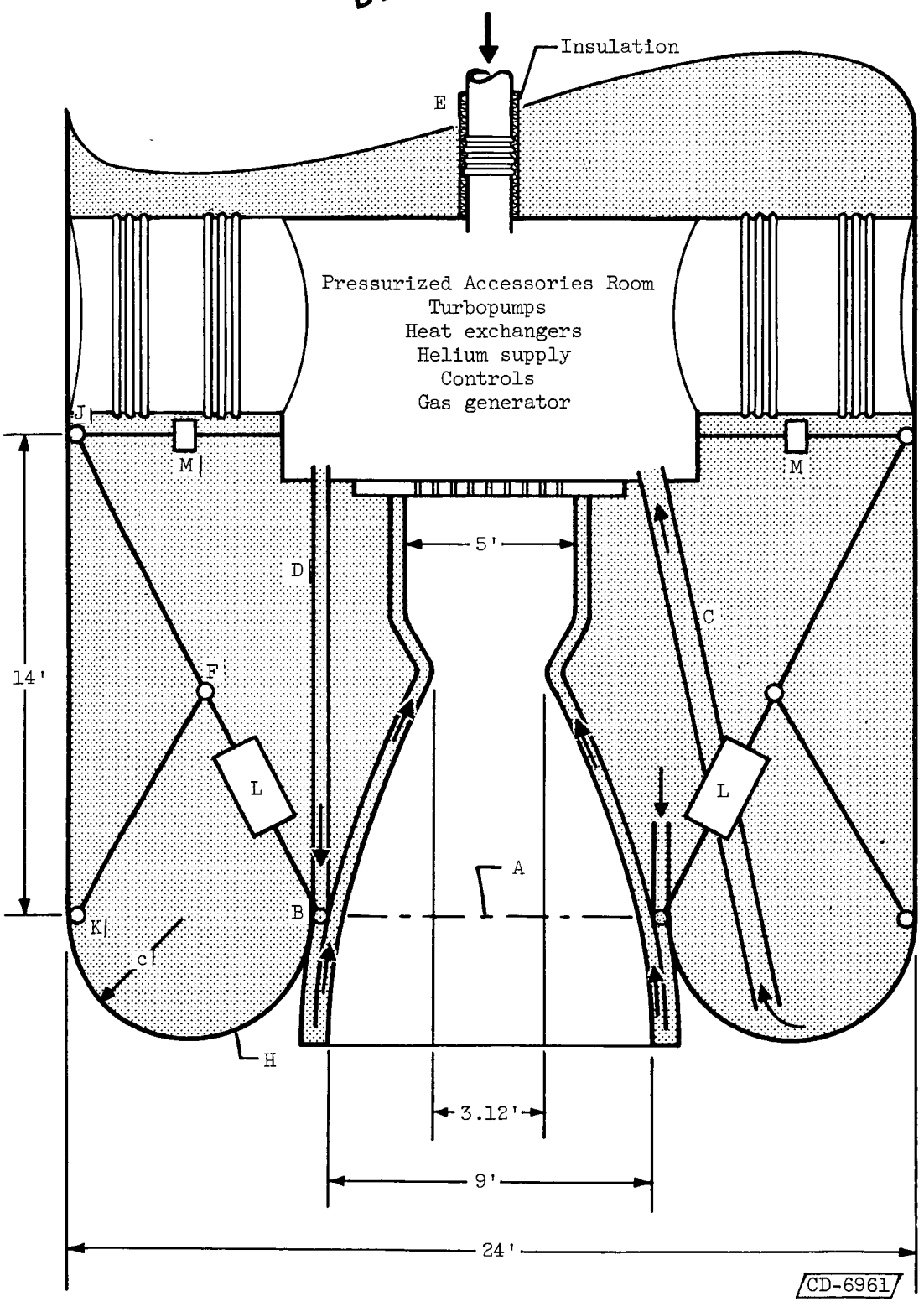

Figure 2. - Lower part of booster hydrogen tank.

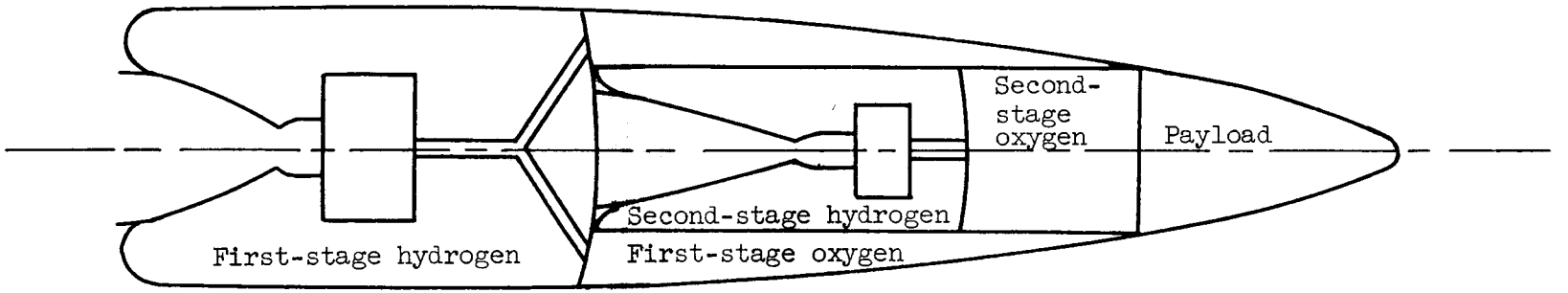

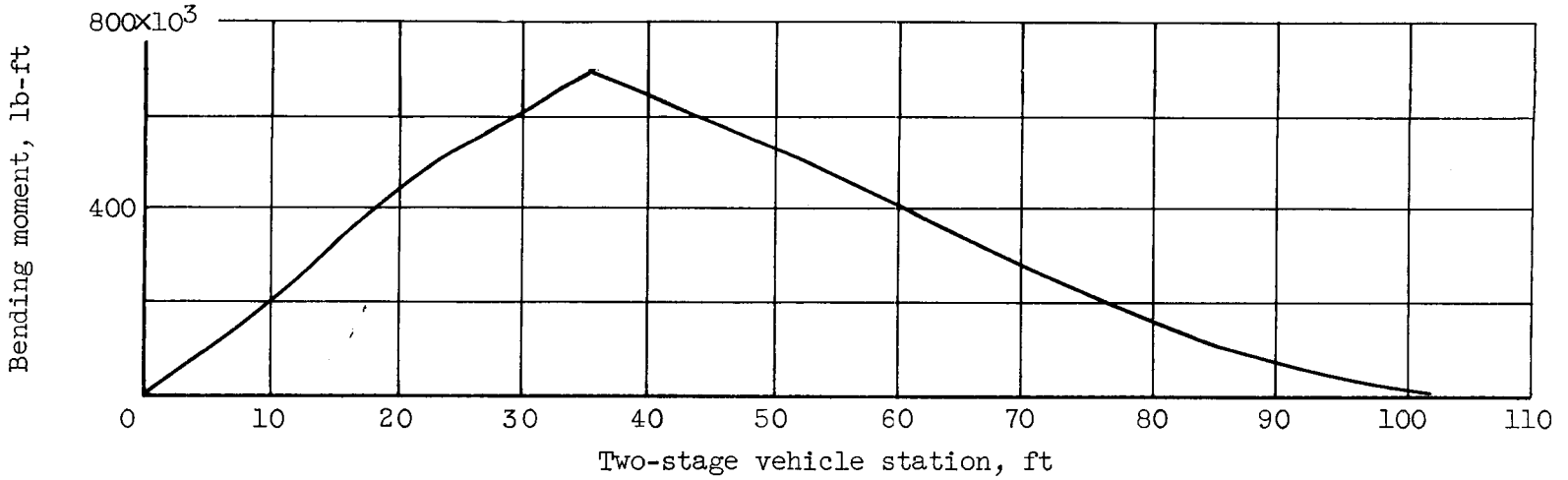

Figure 3. - Bending-moment diagram for most severe combination of required angular acceleration and wind upsetting moments.

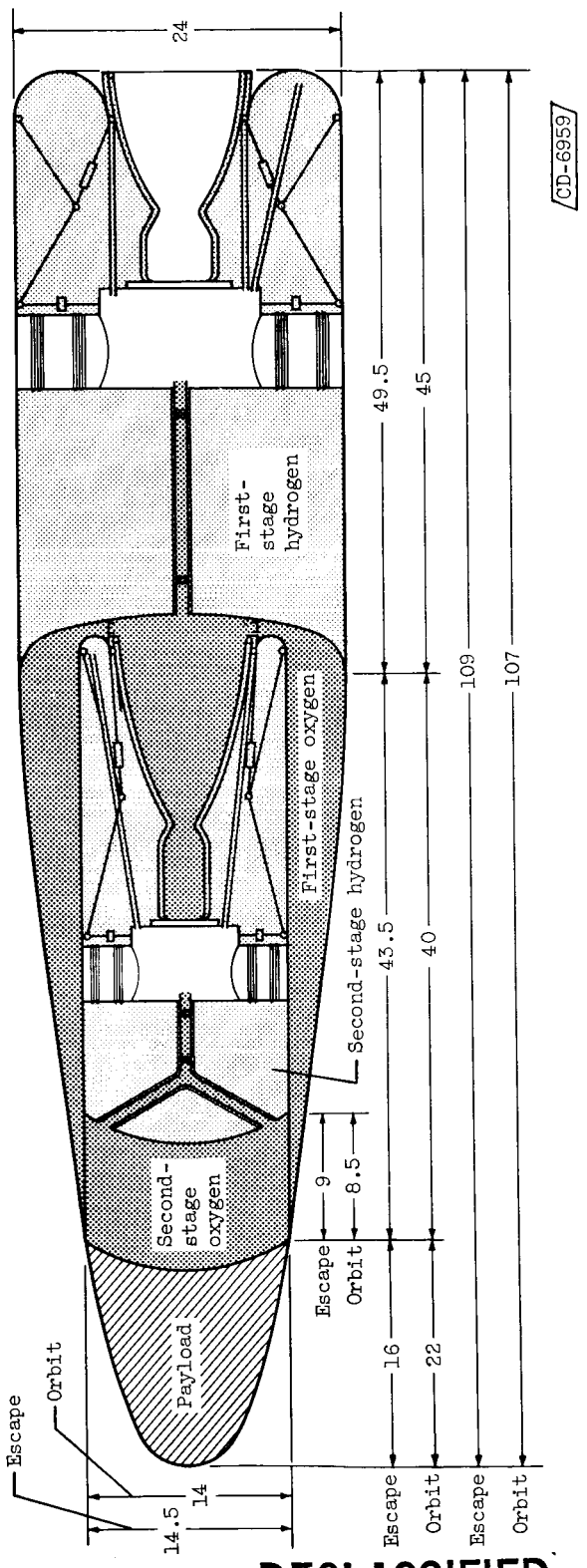

Figure 4. - Two-stage one-million-pound-thrust vehicle. (All dimensions in feet.)

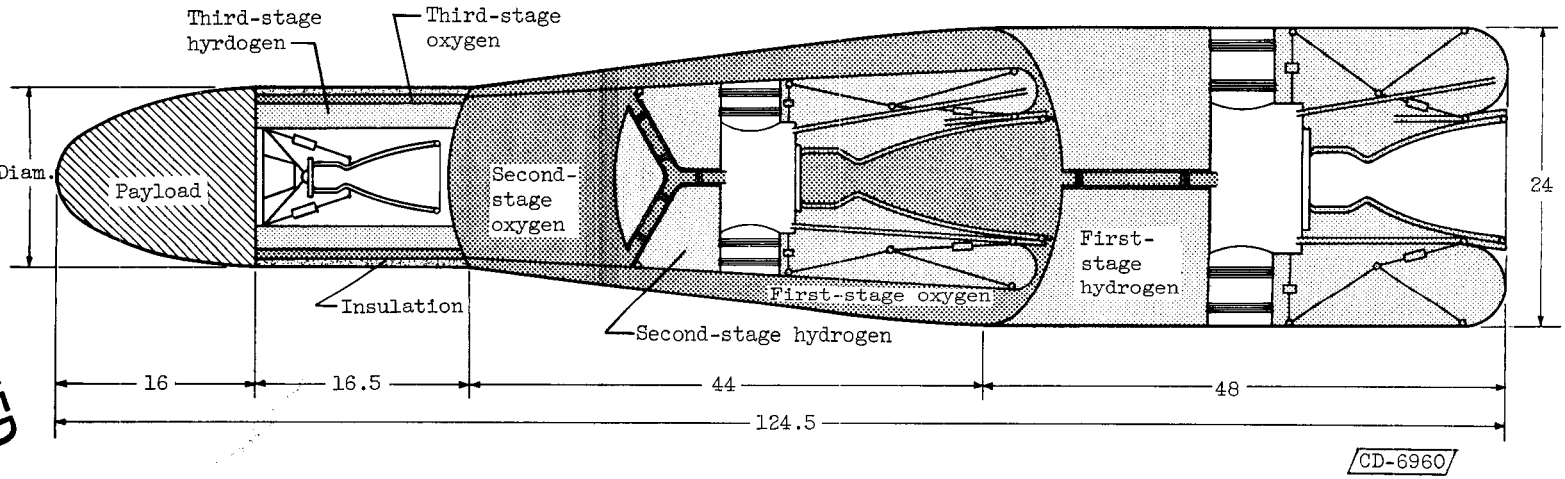

Figure 5. - Three-stage one-million-pound-thrust escape vehicle. (All dimensions in feet.)

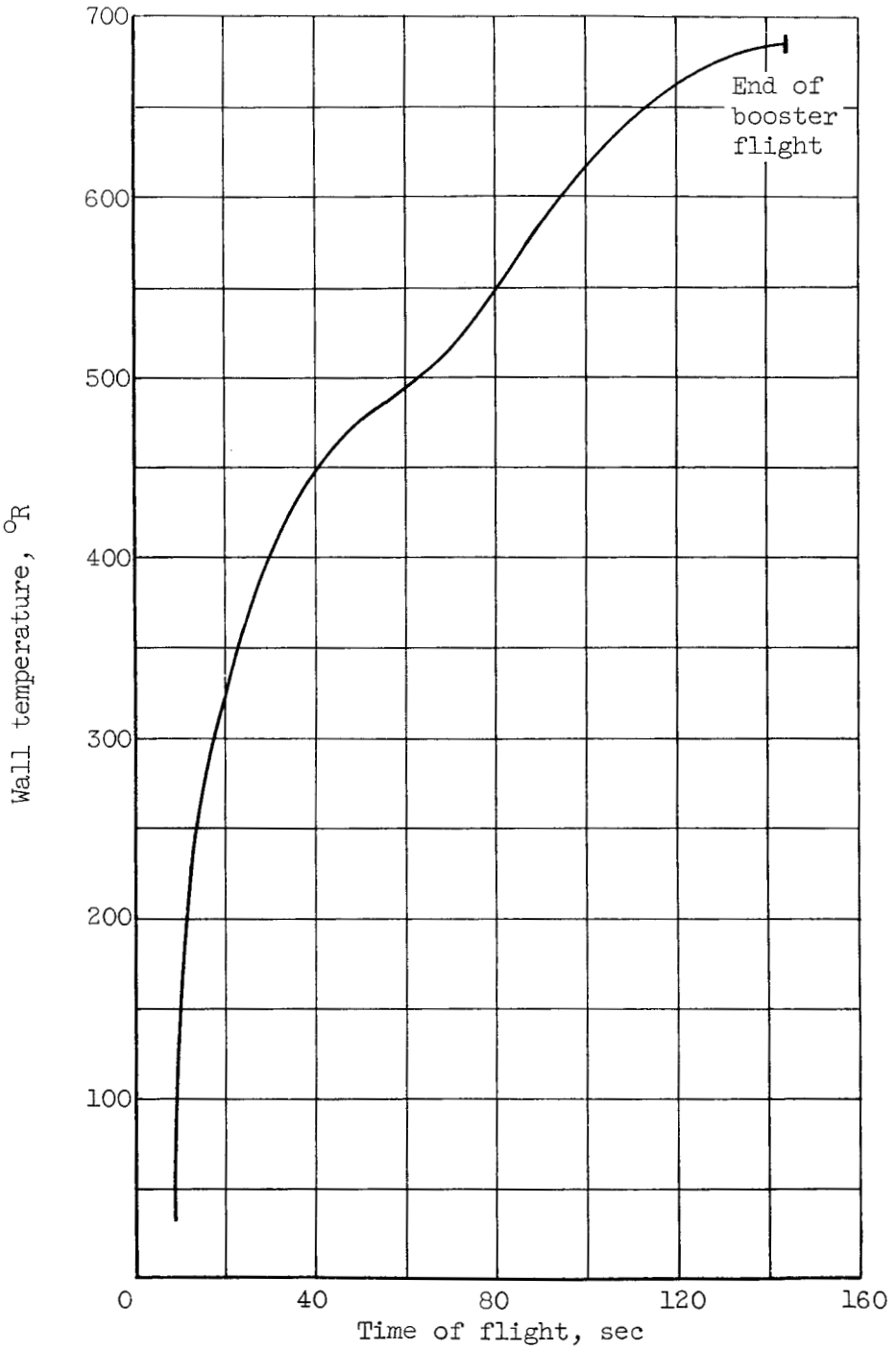

(a) Midway between hydrogen liquid level and oxygen tank bottom.

Figure 6. - Temperature of booster tank wall. Assumes no heat transfer to gas inside tank; all heat absorbed by walls.

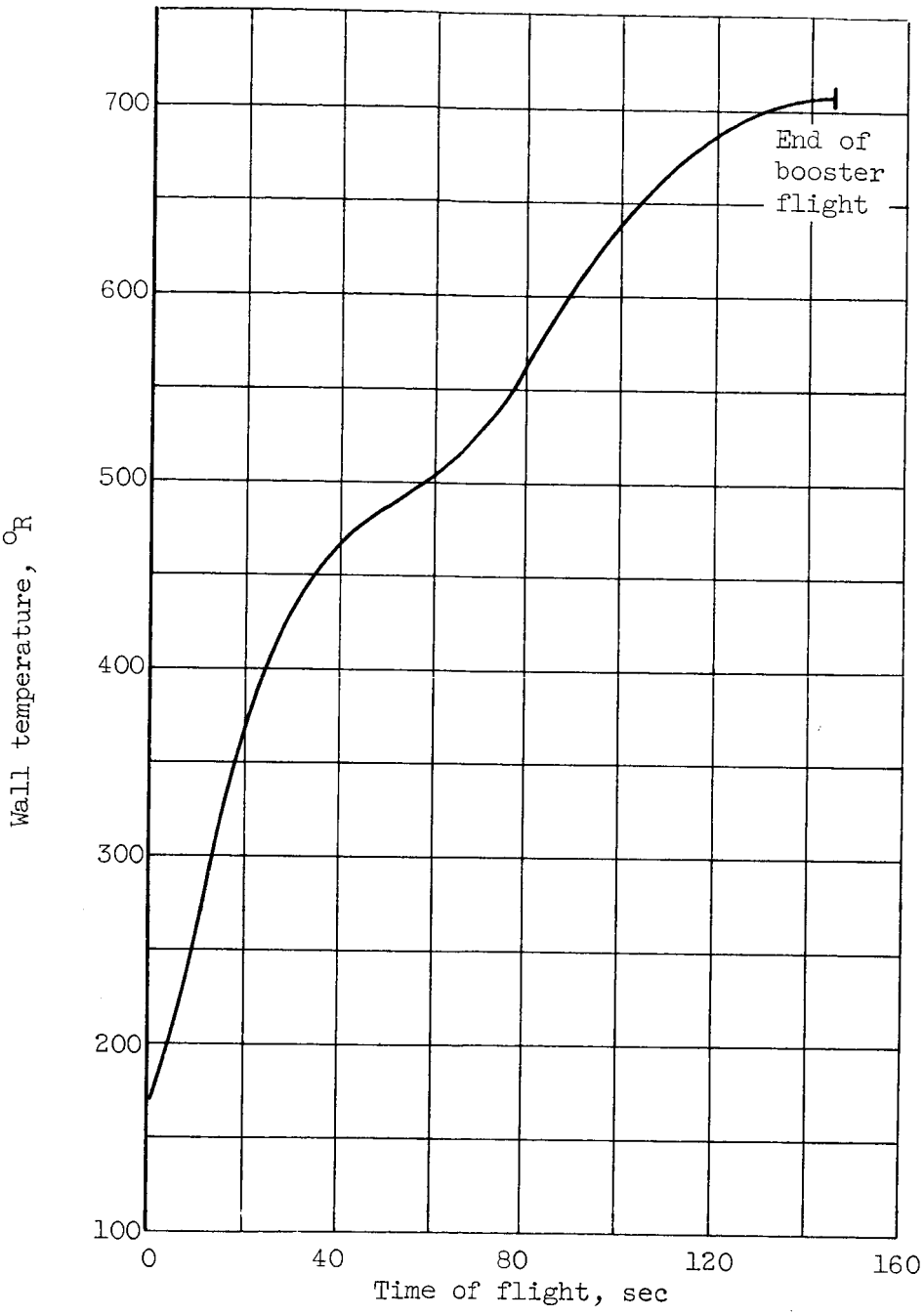

(b) Midway between level of liquid oxygen and top of oxygen tank.

Figure 6. - Concluded. Temperature of booster tank wall. Assumes no heat transfer to gas inside tank; all heat absorbed by walls.

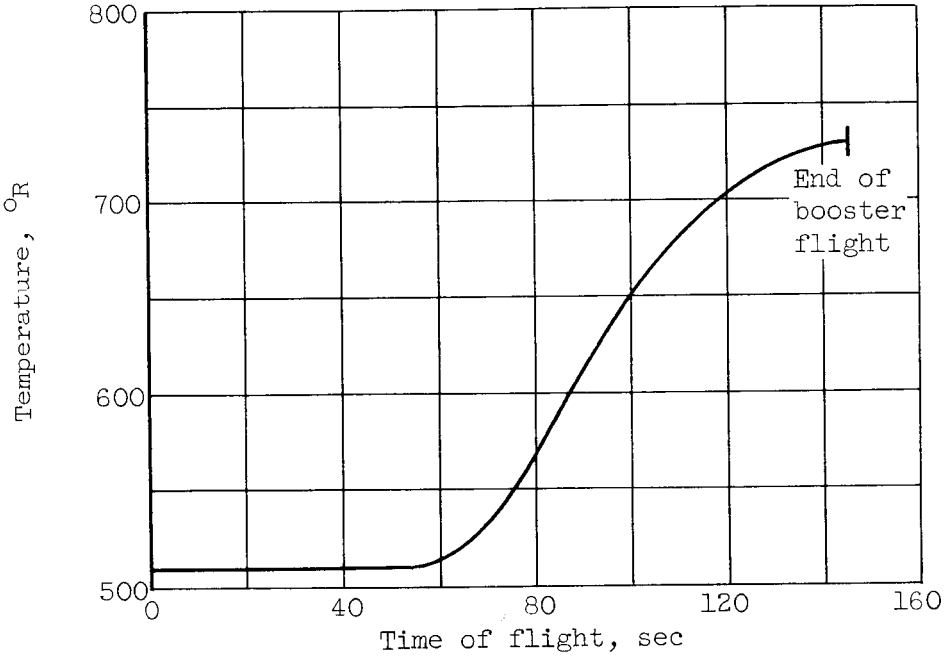

Figure 7. - Skin temperature of foil cover on insulation of third-stage oxygen tank.

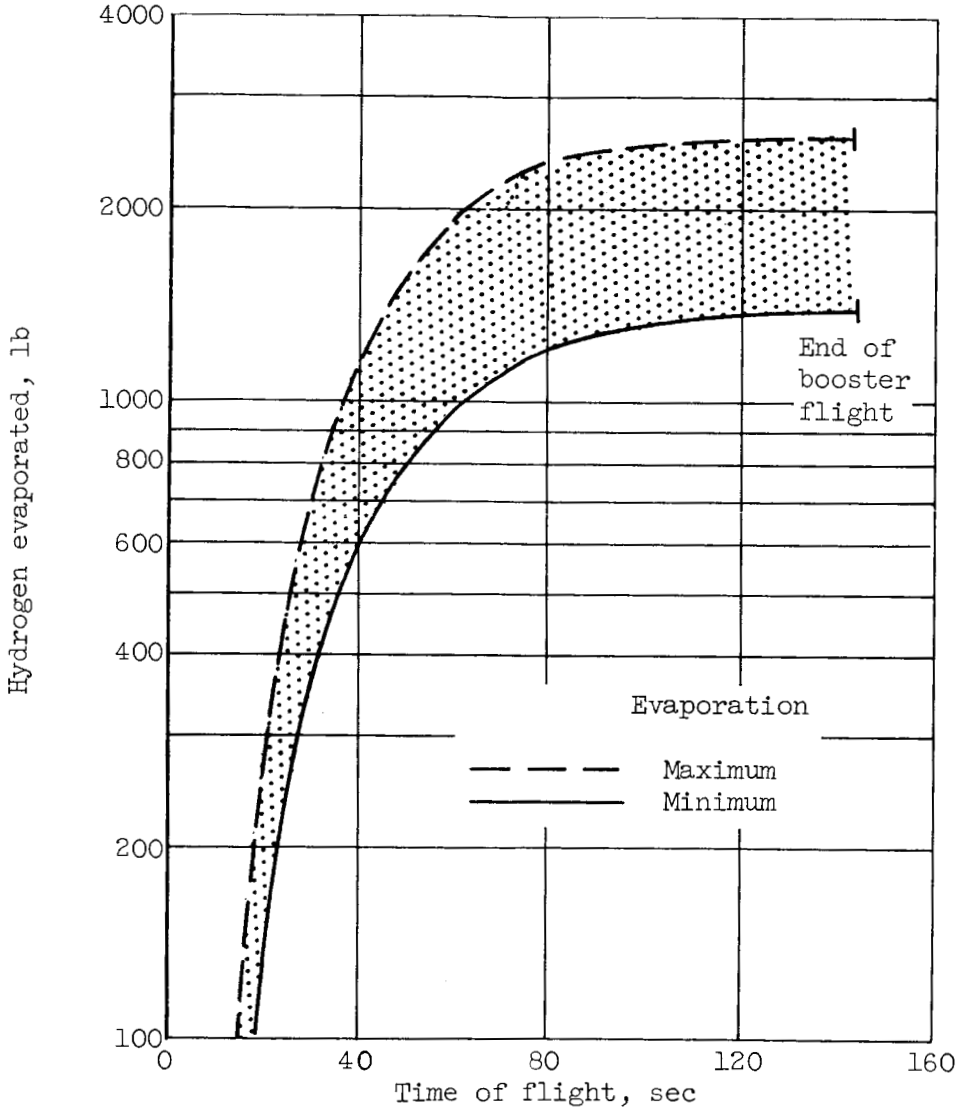

Figure 8. - Cumulative evaporation of hydrogen in booster tank during flight.

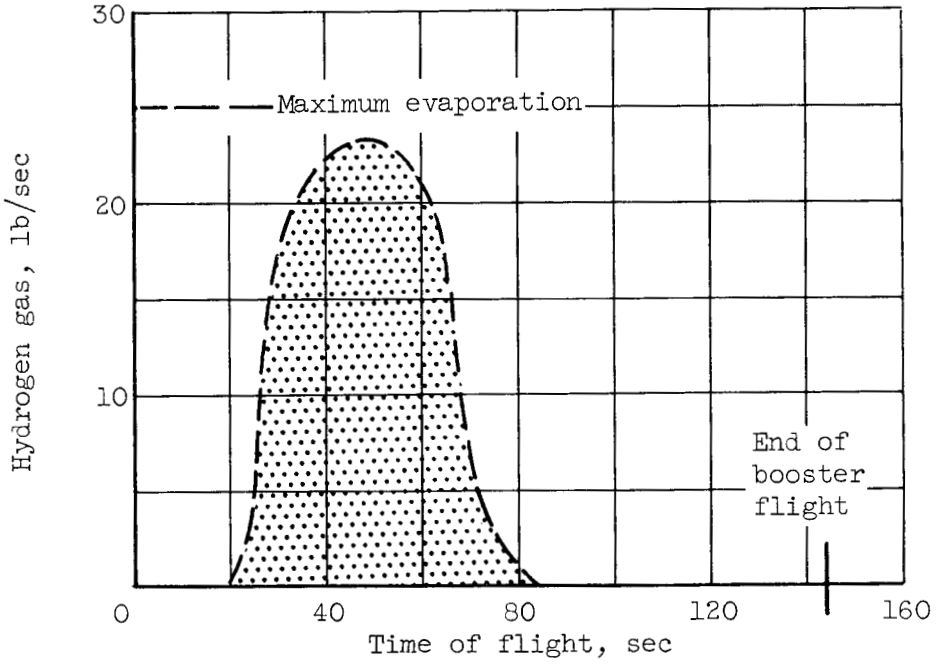

Figure 9. - Maximum possible rate of hydrogen gas valve-off.

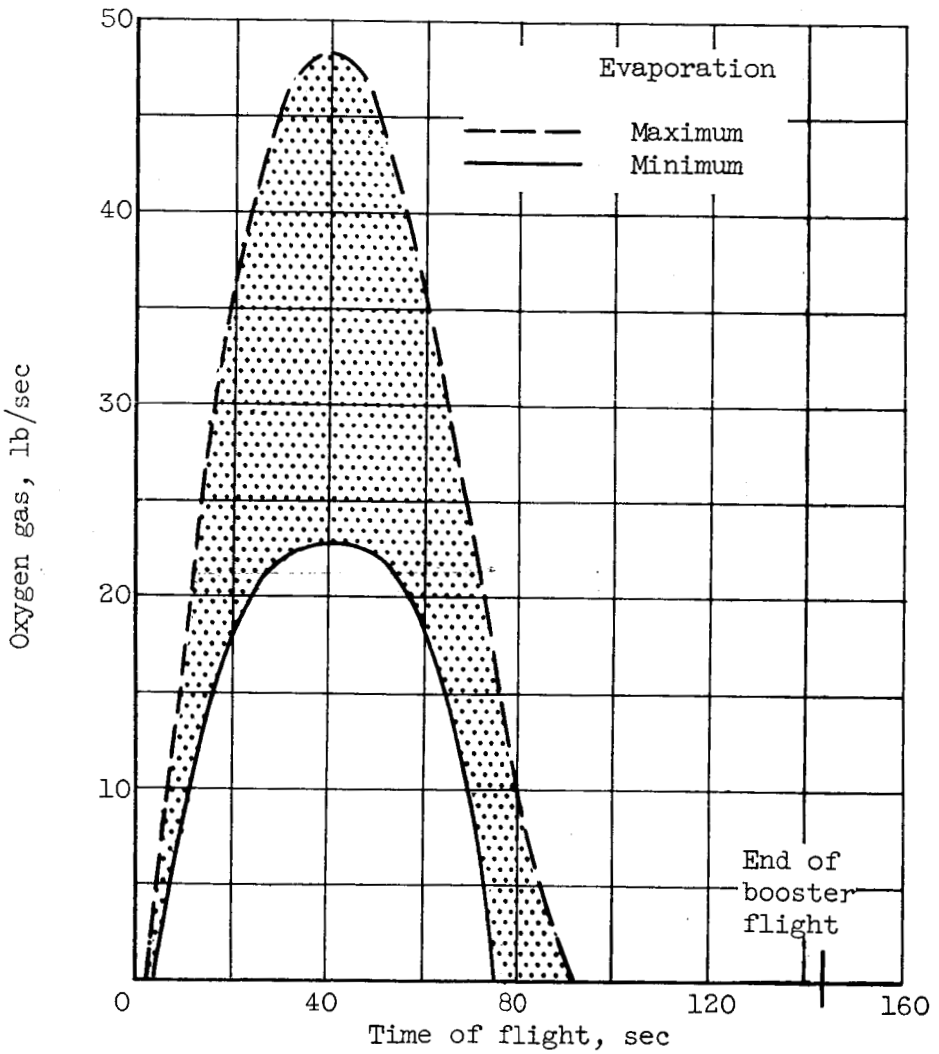

Figure 10. - Maximum and minimum possible rates of oxygen gas valve-off.

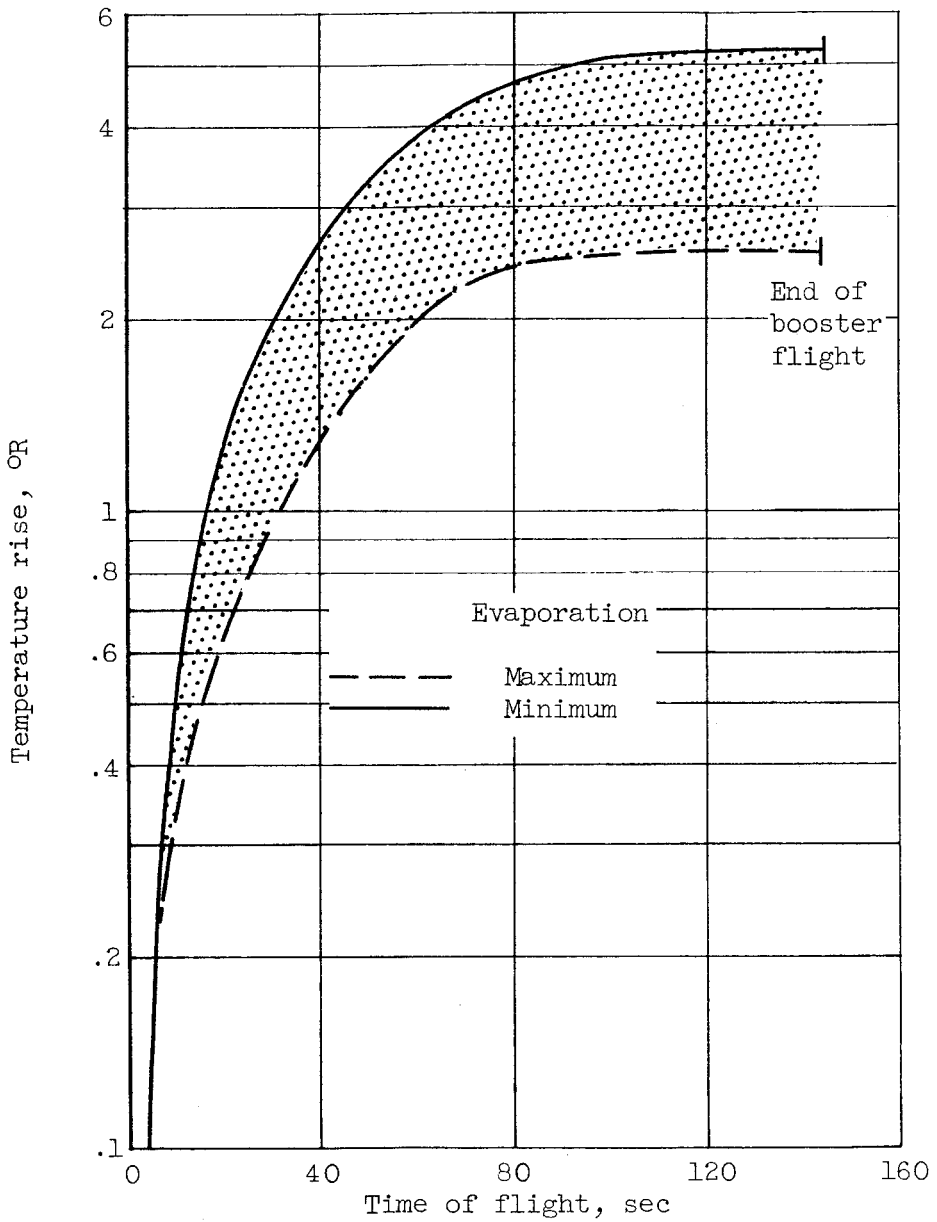

(a) Liquid hydrogen.

Figure 11. - Bulk temperature rise in booster tank during flight.

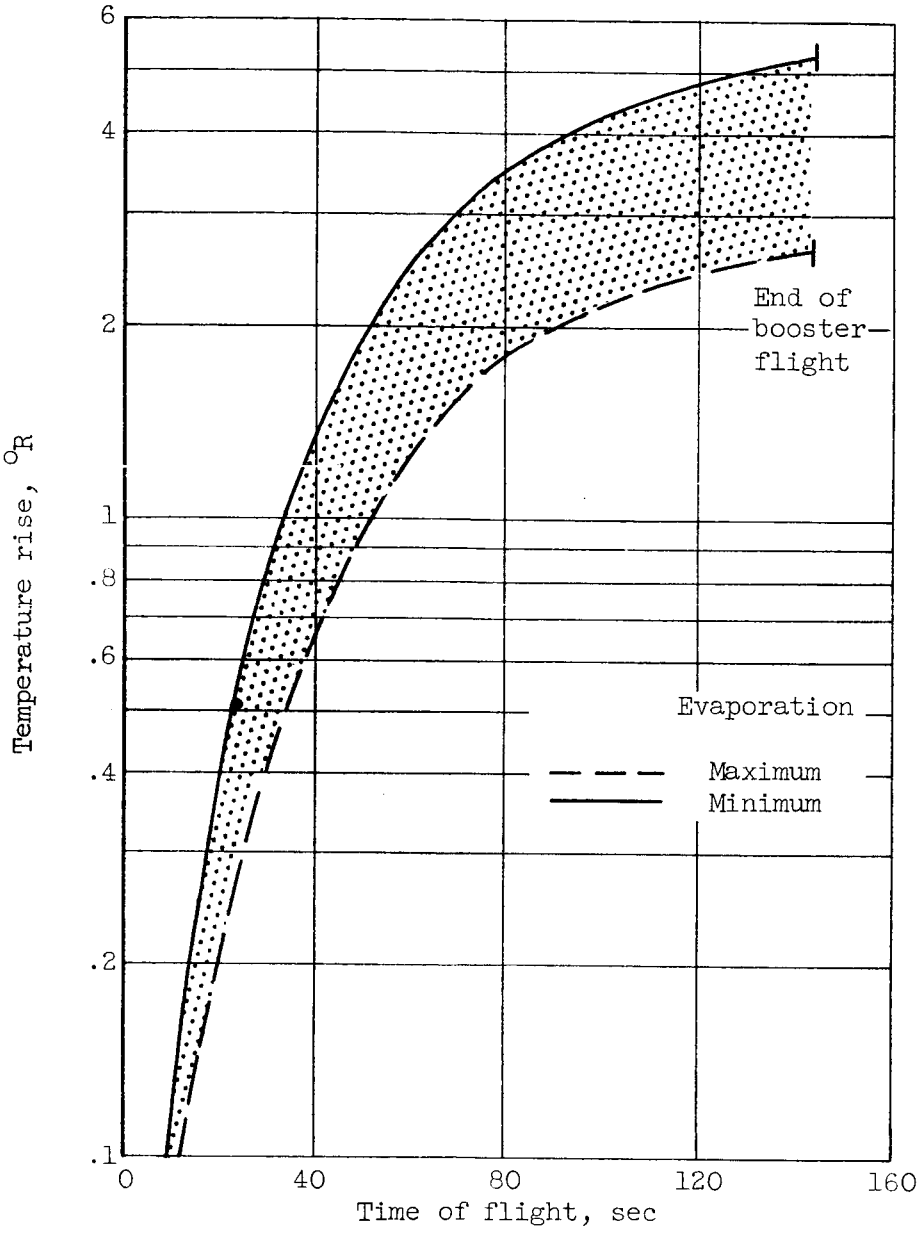

(b) Liquid oxygen.

Figure 11. - Concluded. Bulk temperature rise in booster tank during flight.